



Cr₃C₂-25NiCr Cermet Coating: Preparation, PTFE Sealant, Wear and Corrosion Resistances

Ha Pham Thi¹ · Tuan Nguyen Van¹ · Tuan Anh Nguyen¹ · Quy Le Thu² ·
Ly Pham Thi¹ · Thuy Dao Bich¹ · Trung Trinh Van³ · Cuong Ly Quoc¹

Submitted: 8 October 2020 / in revised form: 11 December 2020 / Accepted: 30 December 2020 / Published online: 20 January 2021
© ASM International 2021

Abstract In this study, Cr₃C₂-25NiCr cermet coatings were fabricated by atmospheric plasma spraying on 304 stainless steel substrate. Then, the coatings were sealed with a Polytetrafluoroethylene (PTFE) emulsion by using two methods: conventional impregnation and ultrasonic vibration. The phase composition, surface morphology, porosity, permeability of PTFE emulsion into the coating, wear and corrosion resistance of the coatings were investigated. The results showed that in the PTFE sealed coatings, besides carbide phases, a PTFE phase with an hexagonal crystal structure was formed. The PTFE covered the surface of the coating. The ultrasonic vibration method increased the permeability of the PTFE emulsion into the coating by more than 2 times that of the conventional impregnation method. The PTFE sealed coating by ultrasonic vibration method had a lower porosity, higher wear and corrosion resistances in 3.5 wt.% NaCl solution than the PTFE coating sealed by conventional impregnation method and PTFE unsealed coating.

Keywords Cr₃C₂-25NiCr · cermet coating · corrosion · plasma spraying · PTFE · wear

Introduction

Corrosion and wear can be considered as the main causes leading to the deterioration of material's properties, thereby causing great damage to the economy. Therefore, it is necessary to find materials that have good corrosion—wear resistance. Many studies show that Cr₃C₂-NiCr thermal spray coatings have high hardness, low friction coefficient and good corrosion—wear resistance (Ref 1–12). In the Cr₃C₂-NiCr coating matrix, while the NiCr alloy component is known as highly corrosion resistant, the presence of Cr₃C₂ brings significant effect in increasing wear resistance. However, the microstructure of Cr₃C₂-NiCr coatings still contains defects such as pores and microcracks. The corrosive media may penetrate into the coating through these defects and cause corrosion to the material, especially when the coatings serve in a severe environment for a long time. In order to reduce porosity and enhance the corrosion—wear resistance of the coating, a simple and effective method is the use of sealing treatment. Besides organic sealants such as epoxy resin, polyurethane resin, and silicone resin, polytetrafluoroethylene (PTFE) is one of the many organic sealants widely used in industry. It has many good properties such as low friction coefficient, good corrosion—wear resistance, relatively high melting point (up to 350°C) and chemical resistance (Ref 13–16).

Studies on PTFE reinforced coatings have also been published in recent years (Ref 17–20). The coefficient of friction for both the PTFE-(Cu-Al) coating and the PTFE-Mo coating was almost constant at a value of 0.1 during the whole sliding distance (Ref 17). The flame and plasma sprayed Al₂O₃ – TiO₂ + 10 wt.% PTFE coatings possessed about two and four times higher wear resistance than AA2024-T6 aluminum alloy substrate, respectively

✉ Tuan Anh Nguyen
ntanh@itt.vast.vn

¹ Institute for Tropical Technology, Vietnam Academy of Science and Technology, 18 Hoang Quoc Viet, Cau Giay, Hanoi, Vietnam

² National Key Laboratory for Welding and Surface treatment Technologies, National Research Institute of Mechanical Engineering, 4 Pham Van Dong, Cau Giay, Hanoi, Vietnam

³ School of Materials Science and Engineering, Hanoi University of Science and Technology, Hai Ba Trung, 1 Dai Co Viet, Hanoi, Vietnam

(Ref 18). The presence of PTFE nanoparticles has contributed to reduce the wear rate of Ni-P coating from $33.07 \times 10^{-6} \text{ mm}^3/\text{Nm}$ to $12.46 \times 10^{-6} \text{ mm}^3/\text{Nm}$ for the Ni-P PTFE containing 10 g/l PTFE and decrease the friction coefficient from 0.64 to 0.2 (Ref 19). The Ni-B coating after 40 wt.% PTFE impregnation can withstand a rubbing test duration of 3600 s with the coefficient of friction less than < 0.1 under both dry sliding and lubricated by 3.5 wt.% NaCl solution (better than the Ni-B coating). In addition, the corrosion resistance of the Ni-B coating on steel substrate is improved after immersion in PTFE (Ref 20). Currently, no studies have been published about the $\text{Cr}_3\text{C}_2\text{-NiCr/PTFE}$ coating.

In this paper, the $\text{Cr}_3\text{C}_2\text{-25NiCr}$ coatings were prepared by atmospheric plasma spraying technique on 304 stainless steel substrate. Then, the coatings were sealed with polytetrafluoroethylene (PTFE) emulsion by using two methods: conventional impregnation and ultrasonic vibration. The effect of the sealing treatment methods by PTFE sealant on the properties of the $\text{Cr}_3\text{C}_2\text{-25NiCr}$ coating, especially the corrosion and wear resistance of the coating were presented and discussed in this study.

Materials and Methods

Materials

In this experiment, $75\text{Cr}_3\text{C}_2\text{-25NiCr}$ powder provided by Wisdom Consumables (Shanghai, China) with the chemical composition of $\text{C} \leq 0.2\%$, $\text{Si} \leq 0.5\%$, 24.5% NiCr and 74.8% Cr_3C_2 was used as the feedstock powder. These particles are spheres with a mean diameter of 20–40 μm (Figure 1). 304 stainless steel plate with the dimensions of 50 mm \times 50 mm \times 5 mm was selected as the substrate. Prior to the spraying, the surfaces of substrates were degreased with acetone and then grit blasted with

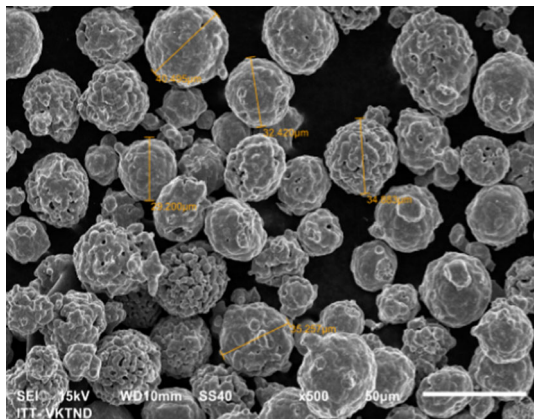


Fig. 1 SEM image of $75\text{Cr}_3\text{C}_2\text{-25NiCr}$ powder (Magnification X500)

corundum to get a surface with a roughness R_z of about 60 μm . 60 wt.% PTFE emulsion (stabilized in water with non-ionic surfactant) from Beijing Starget Chemicals with particle size of 180–250 nm was used as the sealant.

Coating Preparation

The $\text{Cr}_3\text{C}_2\text{-25NiCr}$ coatings on 304 stainless steel substrate were obtained using Tafa 3710-PRAXAIR (US) plasma spray equipment with SG100 torch. The thermal spray parameters are shown in Table 1.

The PTFE emulsion was then continuously stirred using a magnetic stirrer at 1000 rpm during 2 hours. Then, the $\text{Cr}_3\text{C}_2\text{-NiCr}$ coatings were immersed into the PTFE emulsion using two methods as follows:

Conventional impregnation sealing method: The coating was directly immersed into the PTFE emulsion for 5 h at room temperature and atmospheric pressure.

Ultrasonic vibration sealing method: The coating was immersed in the PTFE emulsion and these are placed an ultrasonic vibration bath for 5 h at room temperature and atmospheric pressure.

All the coatings after sealing treatment were heat treated at 120 $^\circ\text{C}$ for 24 hours, 170 $^\circ\text{C}$ for 15 min and 270 $^\circ\text{C}$ for 15 min. Sample labeling is shown in Table 2.

Characterization

The phase composition of the coatings was investigated by x-ray diffraction (XRD, X-RAY D5005/SIEMENS, Germany) at temperature of 25 $^\circ\text{C}$ with $\text{Cu-K}\alpha$ radiation, 2θ angle scanning from 10 $^\circ$ to 70 $^\circ$. The surfaces morphology of the coating and the permeability of PTFE emulsion into the coating were analyzed by scanning electron microscopy coupled with energy dispersive spectroscopy (SEM-EDS, SM-6510LV, Japan). The 3D surface morphology of the coating was analyzed on VHX-600 digital microscope. The porosity of the coating was determined according to the ASTM B276 standard by using the optical microscopy analysis (Axio Observer D1m, Germany). The corrosion

Table 1 Plasma-spraying operating parameters

Plasma-spraying parameters	Value
Arc current, A	600
Primary plasma gas Ar, L/min	70
Secondary plasma gas H_2 , L/min	3
Carrier gas Ar, L/min	5
Spray distance, mm	100
Powder feed rate, g/min	10
Spray angle, $^\circ$	90

Table 2 Types of coating samples (labeling)

Coating samples	Details of cermet coatings
S0	Cr ₃ C ₂ -25NiCr coating without PTFE sealant
SC	PTFE sealed Cr ₃ C ₂ -25NiCr coatings (without ultrasonication during PTFE impregnation)
SU	PTFE sealed Cr ₃ C ₂ -25NiCr coatings (with ultrasonication during PTFE impregnation)

resistance of the coatings in 3.5 wt.% NaCl solution was evaluated by potentiodynamic polarization measurement and electrochemical impedance spectroscopy (EIS) measurement using the VSP-300 multichannel potentiostat/galvanostat (Bio-Logic Science Instruments, France). The electrochemical tests were carried out in a three-electrode cell composed of a sample with an exposed area of 1 cm² as the working electrode, a Pt electrode as counter electrode and a SCE as reference electrode. Experiments were started after immersing the samples into the NaCl solution for 30 minutes. The polarization curves were obtained at a scan rate of 1 mV/s and a scan range of – 500 to 500 mV/SCE around the open circuit potential (E_{ocp}). The corrosion potential and the corrosion current density were obtained through the linear analysis of Tafel approximation. Electrochemical impedance spectroscopy (EIS) measurements were carried out at the open circuit potential (E_{ocp}). The frequency range varied from 10⁻² to 10⁵ Hz with 7 points per decade, potential amplitude $\Delta E = 5$ mV. The wear resistance of the coatings were determined by using UMT-3MT-CETR (US) equipment according to ASTM G133 standard. Wear tests were conducted under the condition of 25 N load, duration of 1000s, oscillating frequency of 5 Hz with stroke of 10 mm at temperature of 25 °C.

Results and Discussion

XRD Analysis

Figure 2 presents the XRD patterns of PTFE and coating samples (S0, SC and SU). As shown in this figure, all three coating samples have phase composition with corresponding crystal structures as follows: Cr₇C₃ (hexagonal), Cr₂₃C₆ (cubic), Ni (cubic), Cr (cubic) và γ -FeNi (cubic) intermetallic phase. The γ -FeNi phase that formed at the steel/coating interface could not have been detected by an x-ray beam incident on the coating surface (due to of the thick sprayed layers > 300 μ m). Thus, Fe might be originated from the powder itself (sprayed dried/sintered powders) or spraying parts. At high temperatures and in an oxidant atmosphere, several reactions can be involved in

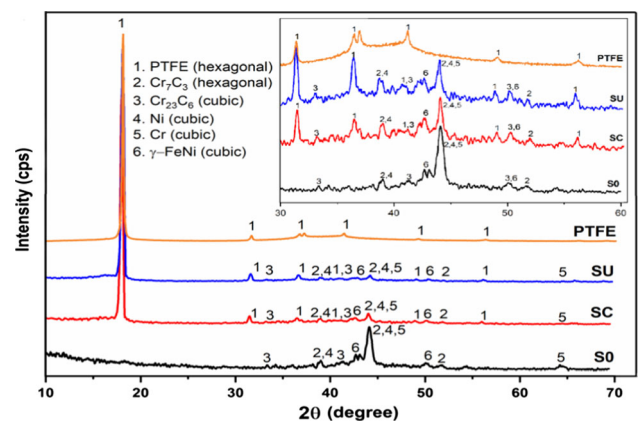
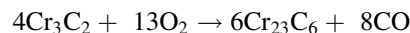
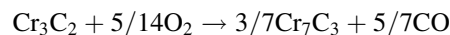
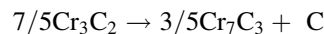


Fig. 2 XRD pattern of the Cr₃C₂-25NiCr coatings

the decomposition of original phases and new phases formation during the spraying process (Ref 1, 3):



However, in case of SC and SU samples, PTFE phase was observed because the PTFE thin film covered most of the coating surfaces. The PTFE phase with hexagonal crystal structure appears at 2θ around 18° with strong intensity and diffraction peaks with lower intensity at 2θ around 31° to 56°, with lattice parameters: $a = b = 5.65540$ Å, $c = 19.508$ Å. In addition, there was no occurrence of diffraction peaks of compounds formed between elements of the coating and PTFE, which showed that the bond between the PTFE and the coating was a mechanical adhesion bond.

Morphological Study

The surface morphology of Cr₃C₂-25NiCr and Cr₃C₂-25NiCr/PTFE coatings at different magnitudes are shown in Fig. 3. Figure 3a shows the surface of S0 sample has high surface roughness with pores and defects. Meanwhile, PTFE has covered almost completely the surfaces of SC and SU samples (Fig. 3b and c). The open pores have disappeared. The surfaces of SC and SU samples are relatively similar.

Fig. 3 SEM images for surface morphologies of various Cr_3C_2 -25NiCr coatings: S0 (a); SC (b) and SU (c) samples

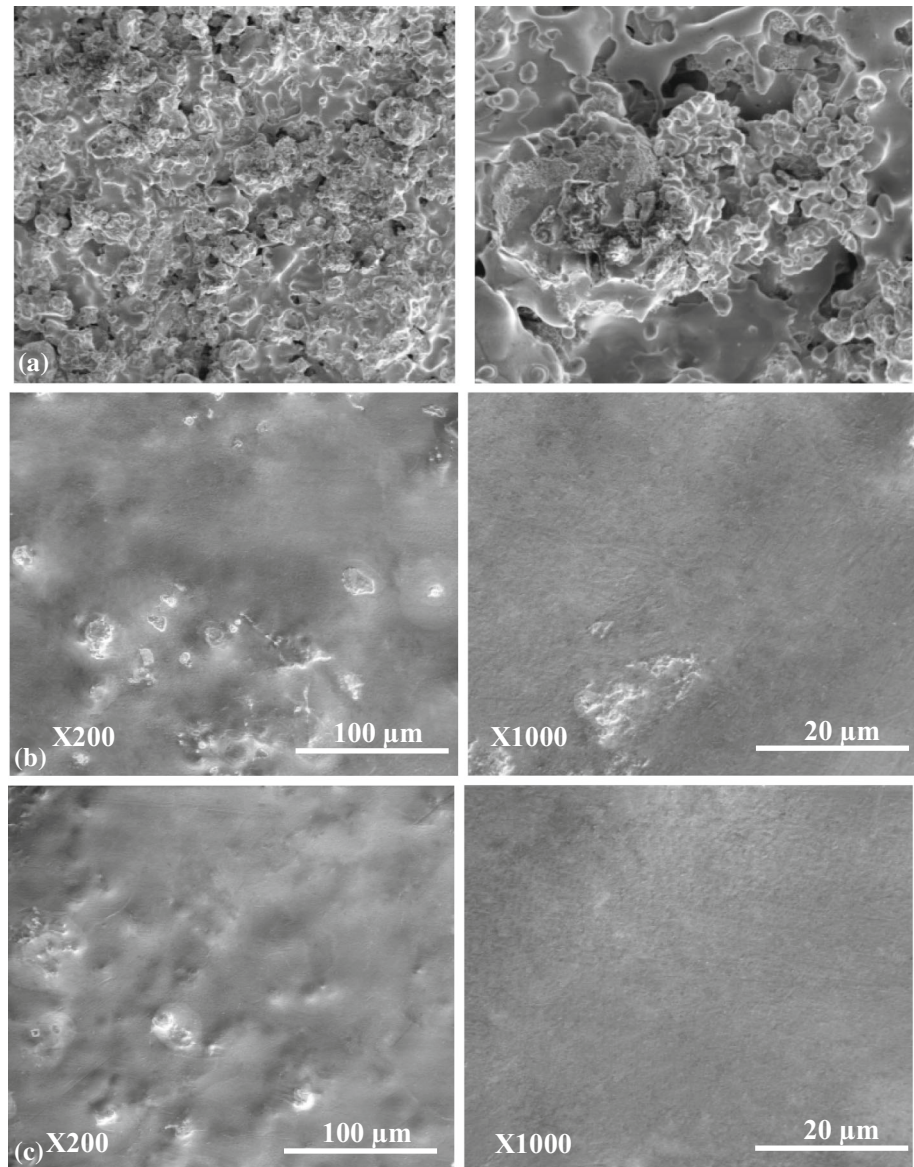


Fig. 4 Three-dimensional surface morphology of the Cr_3C_2 -25NiCr coating

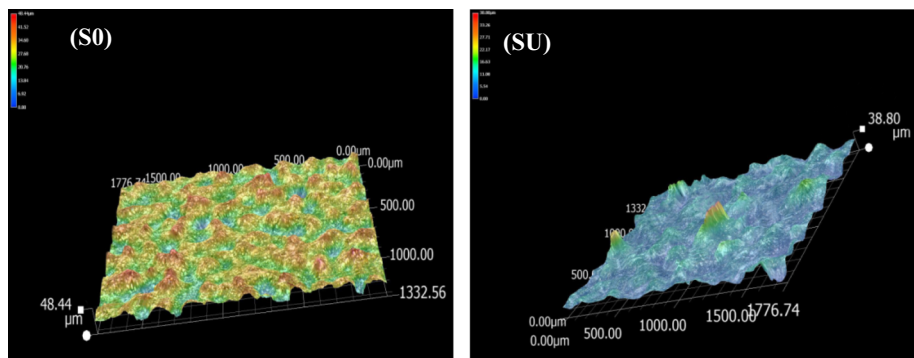


Figure 4 shows the 3D surface morphology of S0 and SU samples. The vertical distance between the lowest point and the highest point on the surface of S0 and SU samples with a rough estimate are about 48 μm and 38 μm ,

respectively. The surface structure of the PTFE sealed coating is more uniform than that of PTFE unsealed coating.

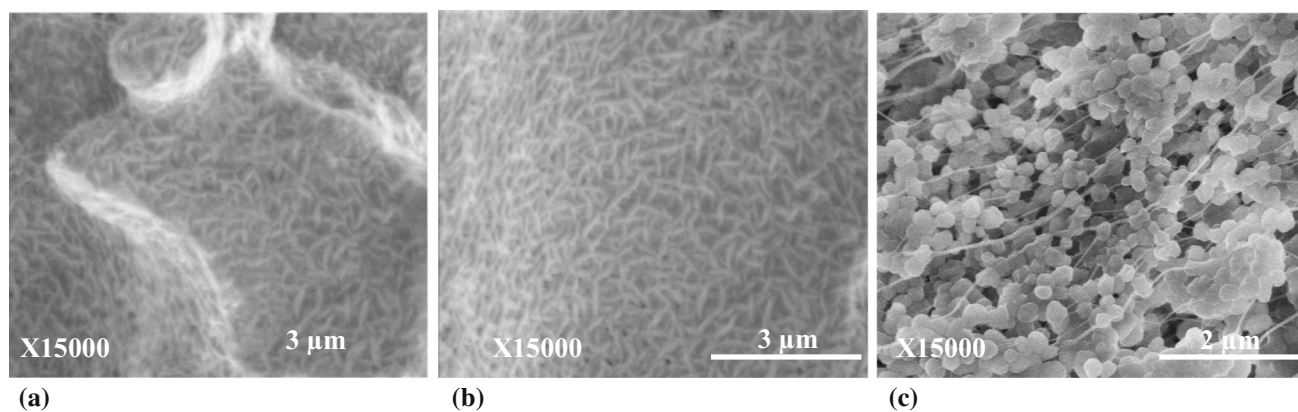


Fig. 5 SEM images of **a** SC coating, **b** SU coating, **c** PTFE, magnification $\times 15000$

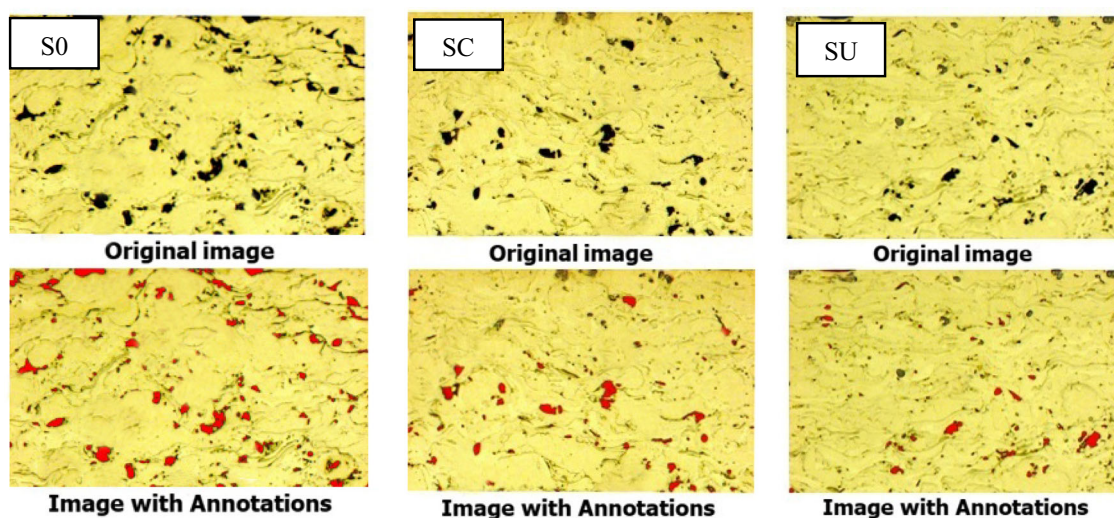


Fig. 6 Cross-sectional images of $\text{Cr}_3\text{C}_2\text{-}25\text{NiCr}$ coating samples (by an optical microscope with magnification X200)

Figure 5a and b shows the surface morphology of the SC and SU coatings, respectively, at high magnification. The PTFE film formed on the surface of the coatings has an interlocking rod shape. Meanwhile, the PTFE particle has a spherical shape (Fig. 5c). Thus, PTFE particles have bonded and formed PTFE film with variable morphology after heat treatment.

The porosity of $\text{Cr}_3\text{C}_2\text{-}25\text{NiCr}$ coatings was measured at three different positions on the cross-sectional microstructure of the coating. Figure 6 presents the cross-sectional structure of all three coatings, and their corresponding porosity was shown in Fig. 7.

The results in Fig. 7 show that the porosity of PTFE sealed $\text{Cr}_3\text{C}_2\text{-}25\text{NiCr}$ coatings has been significantly reduced compared to unsealed $\text{Cr}_3\text{C}_2\text{-}25\text{NiCr}$ coating. The average values of coating porosity decreased in the following order: S0 (3.45%) > SC (2.46%) > SU (1.17%). The ultrasonic vibration method and the conventional impregnation method gives porosity sealing perform of

about 66% and 28 %, respectively. Thus, the ultrasonic vibration method makes the PTFE emulsion to penetrated deeper and fill the pores more than the conventional impregnation method. In order to explain this result, we continued to study the permeability of PTFE emulsion into the coating by the EDS method and explore the mechanism of permeability of PTFE emulsion into the coating.

Permeability of PTFE Emulsion into the Sprayed Coating

The results of SEM-EDS line scan analysis on the cross-section of SC and SU samples (Fig. 8 and 9) show that Cr, Ni, C, F, O and Fe elements are all present in the SC and SU samples. PTFE has the chemical formula $(\text{C}_2\text{F}_4)_n$. The presence of F element in two coatings indicates that PTFE has penetrated inside the coating. The F element in the SC samples was observed up to $\sim 70 \mu\text{m}$ of penetration depth (Fig. 9b), whereas in the SU coating, element F was

detected through a depth of $\sim 150 \mu\text{m}$ (Fig. 9d). On the other hand, the intensity of F element in the SC sample is much lower than the SU sample. These results indicated that the ultrasonic vibration facilitated the penetration of PTFE emulsion throughout the coating with a higher depth and content than that of the conventional impregnation method. This result is completely consistent with the measurement results of the coating porosity.

The mechanism of permeability of PTFE emulsion into the coating has been proposed by Liu et al. (Ref 21). For the conventional impregnation method, the sealing process has been carried out at atmospheric pressure. It was difficult for the sealant to penetrate deeply into the coating because air takes up the place of the pores at the equilibrium pressure environment of a pore system. Therefore, the sealant could not reach the bottom of the pores. However, the sealant could partially penetrate inside by the action of sealant's wettability, which can urge parts of sealing agent into the pores, and thus play a certain role in sealing. As for the ultrasonic vibration method, even smaller cracks and holes could be filled by the sealant, which was mainly contributed by the ultrasonic energy. Ultrasonic cavitation could accelerate the thermal motion, reduced the interfacial tension and improved the compatibility between the

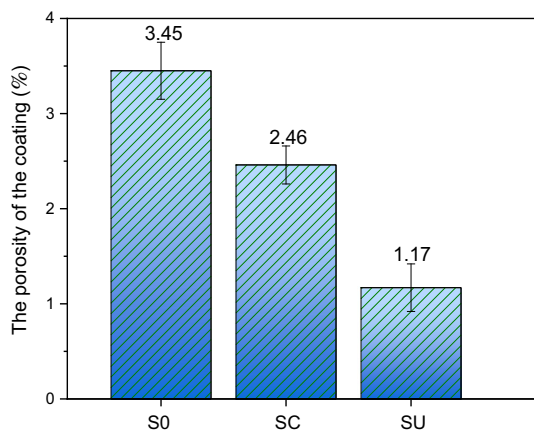
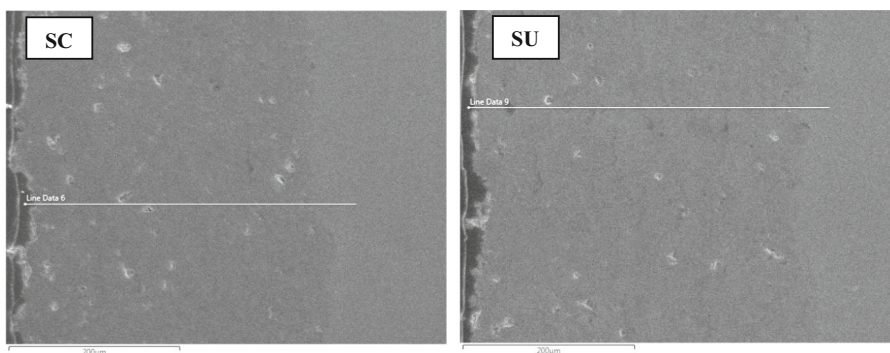


Fig. 7 Porosity of the $\text{Cr}_3\text{C}_2\text{-25NiCr}$ coatings

Fig. 8 Cross-section SEM images of the $\text{Cr}_3\text{C}_2\text{-25NiCr}$ coatings for line scanning



coating and the sealant. It can impel some parts of air within the pores to go into the sealant. At the same time, the escape of the air from the interior of the pores provided room for the sealant, and further facilitates the sealant penetration deep into the inner layer. On the other hand, the residual air inside the sealant continuously escaped due to the combined effect of buoyancy and pressure. This process was repeated and eventually a large amount of sealant was diffused deeper into the coating.

Electrochemical Study

Figure 10 presents the potentiodynamic polarization curves in 3.5 wt.% NaCl solution of these samples. Their values of corrosion potential (E_{corr}) and corrosion current (I_{corr}) are shown in Table 3, respectively. The obtained results showed that the corrosion potential of SU sample (-0.12 V/SCE) was more positive than that of S0 sample (-0.33 V/SCE), SC sample (-0.23 V/SCE) and 304 stainless steel substrate (-0.3 V/SCE). Moreover, SU sample had the lowest corrosion current density. The value of corrosion current density corresponding to S0, SC, SU samples and 304 stainless steel substrate are 0.26, 0.18, 0.08 and $8.24 \mu\text{A}\cdot\text{cm}^{-2}$, respectively. Therefore, SU sample showed the best performance among the coatings to protect the stainless steel substrate against corrosion in NaCl solution.

In addition, the zigzag region in the anode branch of the potentiodynamic polarization curves for the coated samples indicated pitting corrosion and/or attributed to superficial oxide film breakdown (Ref 22).

This is entirely consistent with the results of the EDS line scans and porosity measurements above. PTFE has contributed to filling the pores and defects of SU sample more than SC sample. Thus, the corrosion solution had more difficulty getting absorbed deep into the SU coating.

Figure 11 shows Bode plots of $\text{Cr}_3\text{C}_2\text{-NiCr}$ coatings after 30 minutes of immersion in 3.5 wt.% NaCl solution. The magnitude of the impedance $|Z|$ was plotted as a function of frequency (f). Impedance at the low-frequency region is related to corrosion at the substrate/solution

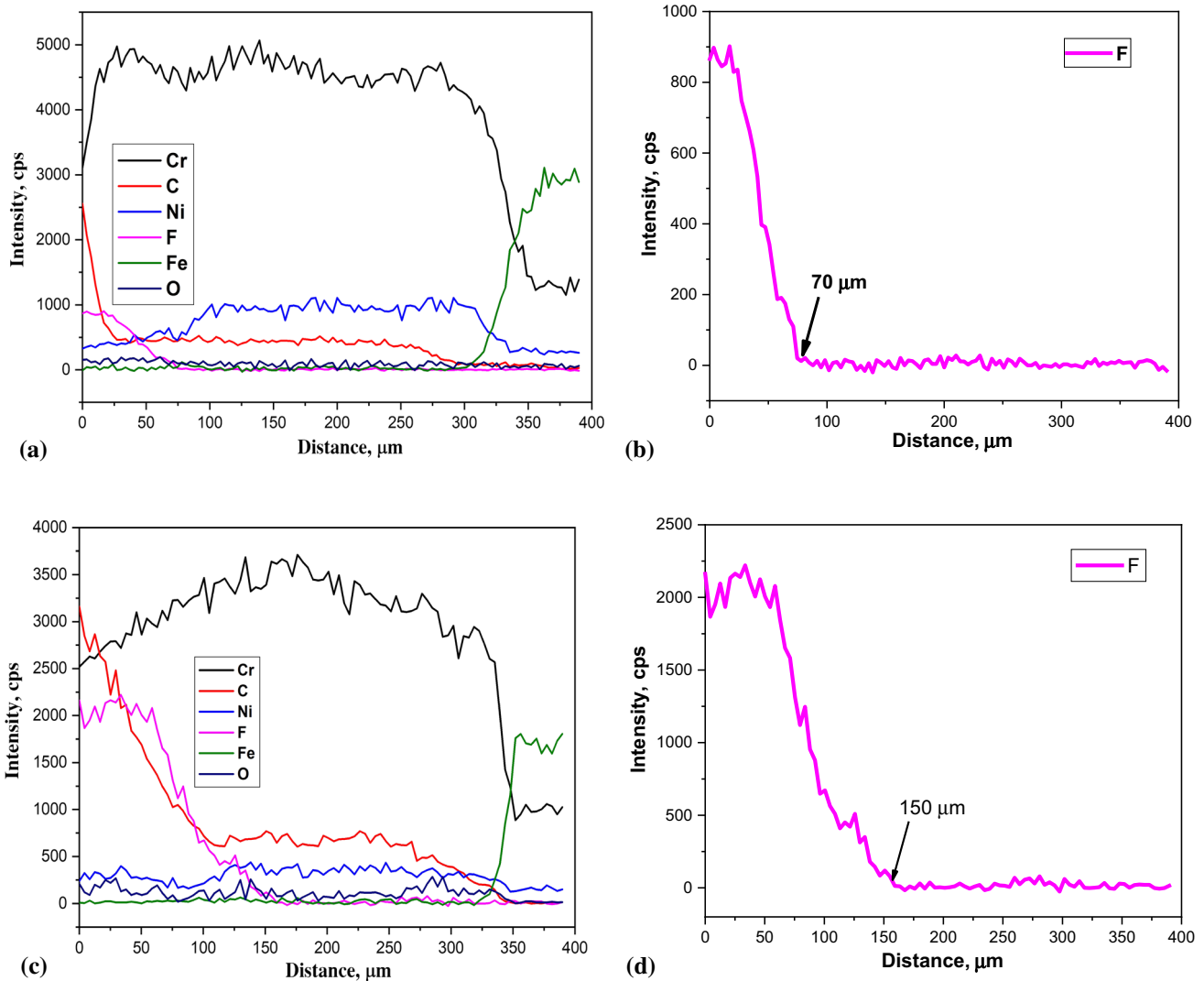


Fig. 9 EDS line scanning of the $\text{Cr}_3\text{C}_2\text{-25NiCr}$ coatings: (a,b) SC and (c,d) SU

interface. These results indicated that at the low frequency, the impedance $|Z|$ of SU sample is approximately 2.3 times greater and 4.9 times greater than that of SC and S0 samples, respectively. Combined with polarization curves results, it can be assumed that PTFE sealed coatings (SC and SU samples) have better corrosion resistant than PTFE unsealed coating (S0) and 304 stainless steel substrate. The PTFE sealed coating by ultrasonic vibration method has the best corrosion resistance in 3.5 wt.% NaCl solution.

Sliding wear resistance

Figure 12 shows the wear depth values of S0, SC and SU samples. As can be seen in this figure, the SC and SU samples have the corresponding wear depth about 43% and 62% lower than the S0 sample. Figure 13 shows the results for the coefficient of friction (COF) as a function of sliding time in dry sliding. The presence of PTFE in the coating

has contributed to reducing the COF of coating. S0 sample shows the COF of approximately 0.25 was observed at the onset of the test, but the COF quickly rises to approximately 0.4 after 1000 s test. Meanwhile, the COF of SC sample increased from 0.13 to 0.17 during the first 300 s of test and remained stable to 700 s of test, then the COF increased to nearly 0.2 at the end of the test. For the SU sample, the COF remained stable around the value of 0.13. Vibration amplitude of COF values during the wear test for the S0 sample is larger than that of the remaining samples due to the surface of S0 has higher roughness.

The obtained wear data can be explained as that when the chrome steel ball moved on the surface of PTFE sealed coating, solid PTFE particles were created between the contact interface of the ball and the coating; therefore, it might form a thin PTFE transfer film on surface of the ball. The PTFE sealed coating became a self-lubricating coating and the ball slides easily on the surface of the coating, thus

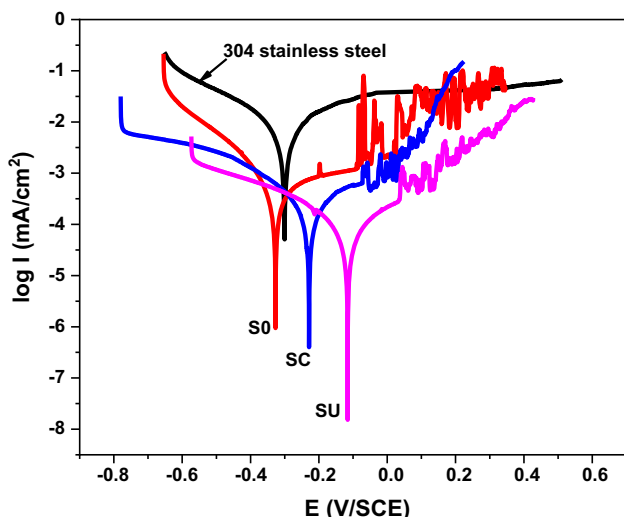


Fig. 10 Polarization curves of Cr₃C₂-NiCr coatings and stainless steel substrate after 30 minutes of immersion in 3.5 wt.% NaCl solution

Table 3 Corrosion parameters of the coating after 30 minutes of immersion in 3.5 wt.%NaCl solution

Sample	E_{corr} , V/SCE	I_{corr} , $\mu A/cm^2$
304 stainless steel	- 0.30	8.24
S0	- 0.33	0.26
SC	- 0.23	0.18
SU	- 0.12	0.08

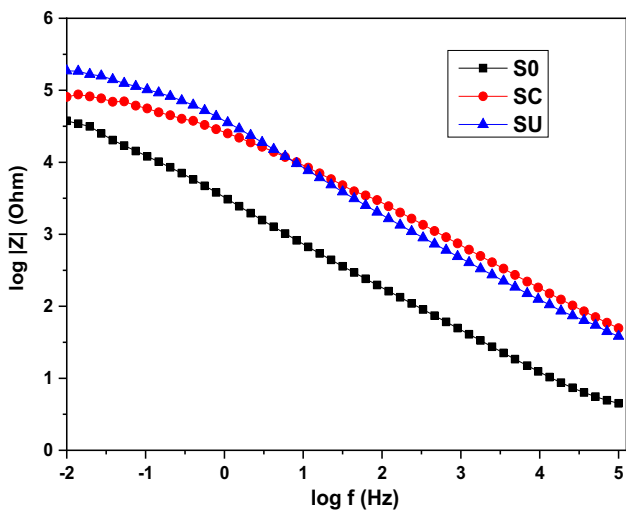


Fig. 11 Bode plots of Cr₃C₂-NiCr coatings after 30 minutes of immersion in 3.5 wt.% NaCl solution

reducing the friction force between the two surfaces resulting leading to reduced wear. For the PTFE sealed coating by the conventional impregnation method, PTFE

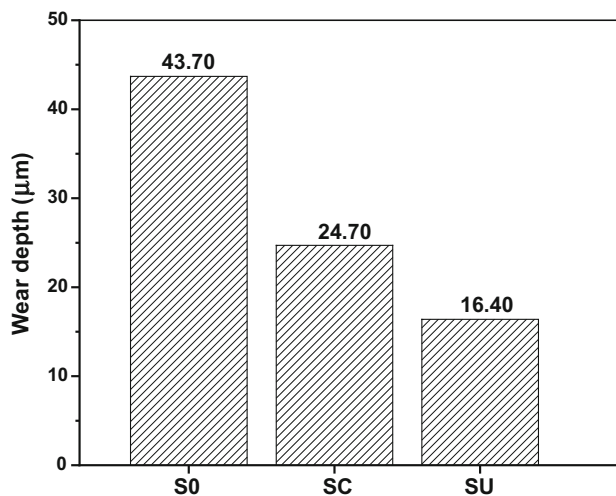


Fig. 12 Wear depth of the Cr₃C₂-25NiCr coatings

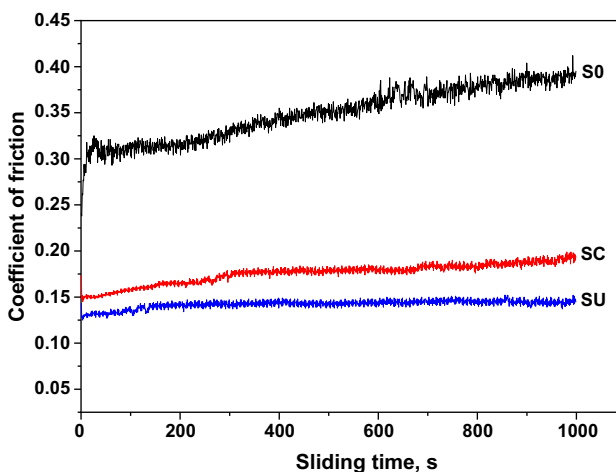


Fig. 13 Friction coefficient of the Cr₃C₂-25NiCr coatings

content that has permeated into the pores and defects of the coating is less than that of the PTFE sealed coating by ultrasonic vibration method. During sliding process, the chrome steel ball was more in contact with the Cr₃C₂-25NiCr coating parts, when the friction force between the two surfaces increase and leading to increase wear compared to the PTFE sealed coating by ultrasonic vibration method.

Thus, from the results of the wear depth and the COF values, the PTFE sealed coating has a higher wear resistance than the PTFE unsealed coating. The PTFE sealed coating by ultrasonic vibration method has the best wear resistance.

Conclusion

The main findings of this research were as follows:

- The surfaces of PTFE-sealed coatings by conventional impregnation and ultrasonic vibration methods are relatively similar and more uniform than that of unsealed coating. PTFE has covered the pores and defects on the surface of coating.
- In the PTFE sealed coatings, besides carbide phases, there is the formation of PTFE phase with hexagonal crystal structure.
- The ultrasonic vibration method increases the permeability of the PTFE emulsion into the coating by more than 2 times that of the conventional impregnation method.
- The PTFE sealed coating by ultrasonic vibration method has lower porosity, higher wear and corrosion resistance in 3.5 wt.% NaCl solution than the PTFE sealed coating by conventional impregnation method and the PTFE unsealed coating.
- Thus, the PTFE sealed Cr₃C₂-25NiCr coating by ultrasonic vibration method is promising for use in environments with corrosive-wear agents.

Acknowledgements The work was supported Vietnam National Foundation for Science and Technology Development (NAFOSTED) under Grant Number 104.03-2019.21 and the Institute of Tropical Technology, Vietnam Academy of Science and Technology (2019 Annual Research Fund).

Data Availability The data used to support the findings of this study are available from the corresponding author upon request.

Conflict of interest The authors declare that there is no conflict of interests regarding the publication of this paper.

References

1. J. Du, F.-Y. Li, Y.-l Li, L.-M. Wang, H.-y Lu, X.-j Ran and X.-y Zhang, Influences of plasma arc remelting on microstructure and service performance of Cr₃C₂-NiCr/NiCrAl composite coating, *Surf. Coat. Technol.*, 2019, **369**, p 16-30.
2. Z. Marcano, J. Lesage, D. Chicot, G. Mesmacque, E.S. Puchi-Cabrera and M.H. Staia, Microstructure and adhesion of Cr₃C₂-NiCr vacuum plasma sprayed coatings, *Surf. Coat. Technol.*, 2008, **202**, p 4406-4410.
3. M. Magnani, P.H. Suegama, N. Espallargas, C.S. Fugivara, S. Dosta, J.M. Guilemany and A.V. Benedetti, Corrosion and wear studies of Cr₃C₂NiCr-HVOF coatings sprayed on AA7050 T7 under cooling, *J. Therm. Spray Technol.*, 2009, **18**(3), p 353-363.
4. A.H. Yaghtina, E. Salahinejad, A. Khosravifarda, A. Araghia and A. Akhbarizadeh, Corrosive wear behavior of chromium carbide coatings deposited by air plasma spraying, *Ceram. Int.*, 2015, **41**, p 7916-7920.
5. M.A. Zavareha, A.A.D.M. Sarhana, B.B. Razaka and W.J. Basirun, The tribological and electrochemical behavior of HVOF-sprayed Cr₃C₂-NiCr ceramic coating on carbon steel, *Ceram. Int.*, 2015, **41**, p 5387-5396.
6. S. Singh, K. Goyal and R. Goyal, Performance of Cr₃C₂-25(Ni-20Cr) and Ni-20Cr coatings on T91 boiler tube steel in simulated boiler environment at 900 °C, *Chem Mater Eng*, 2016, **4**(4), p 57-64.
7. V. Sreenivasulu and M. Manikandan, High-temperature corrosion behaviour of air plasma sprayed Cr₃C₂-25NiCr and NiCrMoNb powder coating on alloy 80 A at 900 °C, *Surf. Coat. Technol.*, 2018, **337**, p 250-259.
8. L. Zhang and J.B. Hou, Study of microstructure and phase of plasma sprayed Cr₃C₂-NiCr coating before and after the sparking plasma sintering, *Phys. Proc.*, 2013, **50**, p 293-296.
9. N. Vashishtha and S.G. Sapate, Abrasive wear maps for high velocity oxy fuel (HVOF) sprayed WC-12Co and Cr₃C₂-25NiCr coatings, *Tribol. Int.*, 2017, **114**, p 290-305.
10. S. Matthews, B. James and M. Hyland, High temperature erosion-oxidation of Cr₃C₂-NiCr thermal spray coatings under simulated turbine conditions, *Corros. Sci.*, 2013, **70**, p 203-211.
11. P.T. Ha, N. Van Tuan, L.T. Quy, N.T. Anh, P.T. Ly, L.Q. Cuong and D.B. Thuy, A study on erosion and corrosion behavior of Cr₃C₂-NiCr cermet coatings, *Vietnam J. Sci. Technol.*, 2018, **56**(3B), p 42-49.
12. T.N. Van, T.A. Nguyen, Q. Le Thu and H.P. Thi, Influence of plasma spraying parameters on microstructure and corrosion resistance of Cr₃C₂-25NiCr cermet carbide coating, *Anti-Corros. Methods Mater.*, 2019, **66**(3), p 336-342.
13. H. Unal, A. Mimaroglu, U. Kadioglu and H. Ekiz, Sliding friction and wear behaviour of polytetrafluoroethylene and its composites under dry conditions, *Mater. Des.*, 2004, **25**(3), p 239-245.
14. W.G. Sawyer and D.L. Burris, Improved wear resistance in alumina-PTFE nanocomposites with irregular shaped nanoparticles, *Wear*, 2006, **260**, p 915-918.
15. C. Ngo Xuan, H.T. Nguyen, Q. Le Thu and T.A. Nguyen, Fabrication of plasma sprayed SiC-Cu cermet coatings, *Kenk. Nanotec. Nanosci.*, 2020, **6**, p 15-33.
16. N. Maqsood, A. Khan, M.K. Alamgir, S.A. Shah and M. Fahad, PTFE thin film coating on 316L stainless steel for corrosion protection in acidic environment, *J. Eng. Appl. Sci.*, 2017, **36**(1), p 183-190.
17. M. Shi, F. Miyazawa, S. Tobe and T.A. Stolarski, The friction and wear properties of PTFE composite-thermal spray metallic binary coatings, *Mater. Trans.*, 2005, **46**(1), p 84-87.
18. H. Mindivan, A study on wear and corrosion behaviour of thermally sprayed alumina-titania composite coatings on aluminium alloys, *Kovove Materialy*, 2010, **48**, p 203-210.
19. H. Rahmati and F. Mahboobi, Studying the effect of the concentration of PTFE nanoparticles on the tribological behavior of Ni-P-PTFE composite coatings, *Iran. J. Oil Gas Sci. Technol.*, 2015, **4**(4), p 67-75.
20. Y. Wan, Y. Yu, L. Cao, M. Zhang, J. Gao and C. Qi, Corrosion and tribological performance of PTFE-coated electroless nickel boron coatings, *Surf. Coat. Technol.*, 2016, **307**(A), p 316-323.
21. M.M. Liu, H.X. Hu and Y.G. Zheng, Effects of three sealing methods of aluminum phosphate sealant on corrosion resistance of the Fe-based amorphous coating, *Surf. Coat. Technol.*, 2017, **309**, p 579-589.
22. L. Fedrizzi, L. Valentinelli, S. Rossi and S. Segna, Tribocorrosion behaviour of HVOF cermet coatings, *Corros. Sci.*, 2007, **49**(7), p 2781-2799.

Publisher's Note Springer Nature remains neutral with regard to jurisdictional claims in published maps and institutional affiliations.